To be submitted to Geophysics

Propagator Matrices for Seismic Waves in Layered Karstic Media

Yingcai Zheng[1], Michael Fehler[1], and Adel Malallah[2]

Yc.zheng@gmail.com

1 Earth Resources Laboratory, Department of Earth, Atmospheric, and Planetary Sciences, Massachusetts Institute of Technology, Cambridge, MA, 02139, USA.
2 Kuwait University

1 Abstract

Seismic imaging methods have been used to locate karstic voids, sinkholes, and clandestine tunnels. To model elastic wave propagation in such media is critical. In this paper, an efficient propagator matrix scheme based on boundary integral equations is proposed to simulate propagation and scattering of elastic seismic waves by karstic voids embedded in a multilayered medium with irregular boundaries, including arbitrary free-surface topography. Each karst can have an arbitrary geometric shape. We used the Burton-Miller formulation to attack the numerical difficulty caused by *fictitious resonance* due to a karstic void. Our method is implemented in the frequency domain and frequency-dependent Q can be readily incorporated. The model is easy to set up and implement and there is no need to mesh the whole computational volume. We validate our method by comparing it to the analytical solution.

2 Introduction

Karsts are formed by dissolution of soluble rocks such as carbonates and evaporate by surface or underground water. A karst can be a dry cavity, or water bearing, or sometimes oil bearing. The karstic topography poses significant challenges in land seismic acquisition and imaging. To image subsurface reservoirs, it is critical to understand the role of karstic topography and deep karsts in scattering seismic waves. This paper proposes a modeling method, which can simultaneously address seismic wave scattering by dry karstic cavities and karstic topography.

For seismic imaging, we need first study how seismic waves are scattered by karsts of arbitrary shapes. For a cylindrical or spherical karst, analytical solutions based on modal expansion exist (e.g., Liu *et al.*, 2000b). These solutions can be used to validate other numerical methods. For a simple rectangular void, finite difference methods or spectral element method (e.g., Gelis *et al.*, 2005; Zeng *et al.*, 2012) can be used to strictly implement the free surface boundary condition. However they suffer from staircase artifacts if the gridding does not conform to the geometry of the real structure. Sometimes, a void is approximated as a low-velocity-low-density material (Xia *et al.*, 2006a; Xia *et al.*, 2006b).

Boundary element methods (BEMs) (e.g., Sanchez-Sesma and Campillo, 1991; Ge *et al.*, 2005; Ge and Chen, 2007; 2008; Ge, 2010; Zheng, 2010), known for their flexibility in dealing with geometries, have been used by many authors (e.g., Benites *et al.*, 1997; Yomogida *et al.*, 1997; Pointer *et al.*, 1998; Liu *et al.*, 2000a; Liu and Zhang, 2000; 2001; Chen *et al.*, 2012) to model seismic wave scattering by cavities in a homogenous medium. However, it is well known that BEMs (direct or indirect) have numerical difficulties for calculating scattering by an inclusion (Burton and Miller, 1971a; Colton and Kress, 1983; Martin, 1990; Bielak *et al.*, 1995; Martin, 2006). For the single layer indirect BEM (IBEM) method, at frequencies (sometimes called *irregular frequencies*) corresponding to the resonant frequencies of the cavity that would have been filled by the same exterior material with a rigid boundary, the boundary integral operators are noninvertible. This property can be shown by the Fredholm theory of integral operators. For a detailed exposition on this issue, we refer to the excellent book by Martin (2006). To make the integral operator invertible, an *ad hoc* solution is to make the frequency complex by adding a small imaginary part to the frequency, which corresponds to modeling the seismic wavefield that decays exponentially in time. When the imaginary part of the frequency is small (i.e., slow decay), the integral operator can still be close to singular. Another solution proposed by Rodriguez-Castellanos *et al.* (2006) is the *multiregion concept*, which splits an inclusion into three regions with overlapping boundaries extending to infinity. However, this technique may not be numerically straightforward when dealing with multiple cavities. A third solution is to complement the original BEMs with the hypersingular BEMs (e.g., Burton and Miller, 1971b; Liu and Rizzo, 1993), which is able to produce numerically stable results for all frequencies. In this paper, we adopt the hypersingular approach.

Despite their obvious advantages and flexibilities, BEM methods are usually limited to solving small problems with small number of discretized boundary elements. This is because the integral operators after boundary discretization become large matrices whose sizes are directionally proportional to the cumulative boundary length. As such, inverting such matrices is computationally intensive and therefore BEM is limited to problems with a few boundaries.

Earlier propagator-matrix methods such as the discrete wavenumber method based on indirect BIE (e.g., Bouchon and Campillo, 1989) using single layer potentials can handle irregular-layered media with multiple boundaries. However, since it uses global Fourier transform between space and wavenumber domains, the geometry of the internal boundary needs to be simple and single-valued with respect to one coordinate. Recently, Ge and Chen (2008) using direct BEM and Liu *et al.* (2008) using indirect BEM, independently, proposed essentially similar space-domain propagator-matrix method to simulate waves in irregularly layered media with any number of layers. However, the mathematical formulation of this idea is not applicable if a layer contains karstic voids or inclusions The key of their method is to establish an integral relation between displacement and traction on each boundary. But for the karst surface, such a relation is not always possible when the frequency corresponds to one of the fictitious resonant frequencies of the cavity. However, we show that by using the Burton-Miller formulation and adding the hypersingular BIE, such a relation can always be established for the cavity surface. It is the aim of our paper to firmly establish this relation on the karst surface.

3 Theory and Method

We first review some basics of the boundary integral equation. Later we will show that these BIEs can be used to build propagator matrices.

The BIE for the interior domain V_I (Figure 1.) reads

$$\frac{1}{2}u_n(\mathbf{x}') = u_n^0(\mathbf{x}') - \oiint_S \left[u_i(\mathbf{x}) T_{in}^{\nu}(\mathbf{x},\mathbf{x}',\omega) - G_{in}(\mathbf{x},\mathbf{x}',\omega)\mathbf{t}_i(\mathbf{x}) \right] dS(\mathbf{x}), \quad \mathbf{x},\mathbf{x}' \in S \tag{1}$$

where $G_{ij}(\mathbf{x}\,|\,\mathbf{x}')$ is the interior elastic Green's function for a receiver at $\mathbf{x}$ and a point force $\mathbf{f}$ at $\mathbf{x}'$, $\mathbf{f} = \mathbf{e}_j \delta(\mathbf{x}-\mathbf{x}')$, in the frequency domain. The force direction is $\mathbf{e}_j$, the unit vector along j-th axis and the receiver polarization is along the i-th axis. The interior Green's traction tensor $T_{in}^{\nu}(\mathbf{x}\,|\,\mathbf{x}')$ is the i-th component traction for a surface element with outward normal ν at $\mathbf{x}$ for a point force at $\mathbf{x}'$ in the frequency domain. The point force is along j-th axis. In operator form, equation (1) reads:

$$\frac{1}{2}\mathbf{u} = \mathbf{u}^0 - A\mathbf{u} + B\mathbf{t}\ , \tag{2}$$

which expresses a relation between surface displacement $\mathbf{u}$ and traction $\mathbf{t}$:

$$\mathbf{u} = \left[I/2 + A\right]^{-1} B\mathbf{t} + \left[I/2 + A\right]^{-1} \mathbf{u}_0\ . \tag{3}$$

However, $\left[I/2 + A\right]^{-1}$ does not exist if the frequency ω is an eigen frequency of the interior problem with a free surface boundary condition on S. This is well known (Rodriguez-Castellanos *et al.*, 2006). In the eigen state, there are non-zero eigen functions $\mathbf{v}_k$'s which satisfy

$$\left[I/2 + A\right]\mathbf{v}_k = 0, \quad k = 1,2,\cdots. \tag{4}$$

The eigen functions $\mathbf{v}_k$ is called a normal mode. This can cause nonuniqueness for $\mathbf{u}$ in equation (2) and it has been well known. To remedy this, one needs to use the hypersingular BIE which is

constructed by taking spatial derivative of equation (1) with respect to $\mathbf{x}'$ and then convert $\nabla_{\mathbf{x}'}\mathbf{u}(\mathbf{x}')$ to traction vector $\mathbf{t}(\mathbf{x}')$ with surface normal $\nu(\mathbf{x}')$ using Hooke's law:

$$\frac{1}{2}t_n(\mathbf{x}') = t_n^0(\mathbf{x}') - \oiint_S \left[u_i(\mathbf{x})H_{in}^{\nu'\nu}(\mathbf{x},\mathbf{x}',\omega) - K_{in}^{\nu'}(\mathbf{x},\mathbf{x}',\omega)\mathbf{t}_i(\mathbf{x})\right]dS(\mathbf{x}), \quad \mathbf{x},\mathbf{x}' \in S\,. \tag{5}$$

where It is understood that in both (1) and (5), the surface integral are in the sense of Cauchy principal value. Write equations (1) and (5) in operator form:

$$\frac{1}{2}\mathbf{t} = \mathbf{t}^0 - H\mathbf{u} + K\mathbf{t}\,. \tag{6}$$

It is shown (Burton and Miller, 1971b) that if we linearly combine equations (2) and (6)

$$\frac{1}{2}(\mathbf{u} + i\gamma\mathbf{t}) = \mathbf{u}^0 + i\gamma\mathbf{t}^0 - (A + i\gamma H)\mathbf{u} + (B + i\gamma K)\mathbf{t} \tag{7}$$

where $\gamma \in \mathbb{R}$ and $\gamma \neq 0$. There is a unique relation between $\mathbf{u}$ and $\mathbf{t}$ on S for the exterior bie:

$$\mathbf{u} = \left[\mathbf{I}/2 + A + i\gamma H\right]^{-1}(B + i\gamma K)\mathbf{t} + \left[\mathbf{I}/2 + A + i\gamma H\right]^{-1}\left(\mathbf{u}^0 + i\gamma\mathbf{t}^0\right). \tag{8}$$

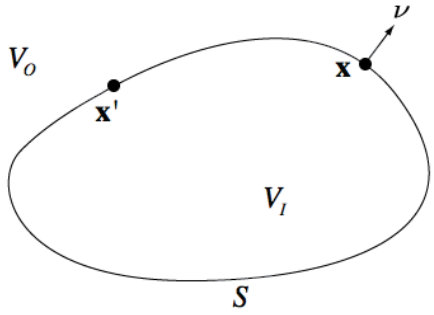

Figure 1. A finite domain V_I bounded by surface S with infinite exterior domain V_O. The outward surface normal at a surface point $\mathbf{x} \in S$ is $\nu = \nu(\mathbf{x})$.

Next we build propagator matrix using the BIEs. We consider a multilayered medium (`Figure 2`). Each interface can be closed such as the spherical Earth or open. The first interface can be the free surface. The wavefield below the last interface satisfies the Sommerfeld radiation condition. On each interface, we use $\mathbf{u}_i$ and $\mathbf{t}_i$ to denote displacement and traction, respectively. Our objective here is to show a fact that $\mathbf{u}_i$ and $\mathbf{t}_i$ are related uniquely to each other by a matrix. This has been observed for general multilayered medium without inclusions (Ge and Chen, 2007; 2008). With inclusions, this relation still holds provided one can solve the difficulty caused by resonance due to the inclusion.

3.1 Last layer

In last layer N, we have

$$\frac{1}{2}\mathbf{u}_N = -A_N\mathbf{u}_N + B_N\mathbf{t}_N - A_{N\Gamma}\mathbf{u}_\Gamma + B_{N\Gamma}\mathbf{t}_\Gamma + \mathbf{u}_N^0. \tag{9}$$

$$\frac{1}{2}\mathbf{u}_\Gamma = -A_{\Gamma N}\mathbf{u}_N + B_{\Gamma N}\mathbf{t}_N - A_{\Gamma\Gamma}\mathbf{u}_\Gamma + B_{\Gamma\Gamma}\mathbf{t}_\Gamma + \mathbf{u}_\Gamma^0 \tag{10}$$

$$\frac{1}{2}\mathbf{t}_\Gamma = -H_{\Gamma N}\mathbf{u}_N + K_{\Gamma N}\mathbf{t}_N - H_{\Gamma\Gamma}\mathbf{u}_\Gamma + K_{\Gamma\Gamma}\mathbf{t}_\Gamma + \mathbf{t}_\Gamma^0 \tag{11}$$

We can linearly combine equations (10) and (11) and get

$$\frac{1}{2}\left(\mathbf{u}_\Gamma + \gamma\mathbf{t}_\Gamma\right) = -\tilde{A}_{\Gamma N}\mathbf{u}_N + \tilde{B}_{\Gamma N}\mathbf{t}_N - \tilde{A}_{\Gamma\Gamma}\mathbf{u}_\Gamma + \tilde{B}_{\Gamma\Gamma}\mathbf{t}_\Gamma + \tilde{\mathbf{u}}_\Gamma^0 \tag{12}$$

where

$$\begin{aligned}
\tilde{A}_{\Gamma N} &= A_{\Gamma N} + \gamma\tilde{H}_{\Gamma N}, \\
\tilde{B}_{\Gamma N} &= B_{\Gamma N} + \gamma\tilde{B}_{\Gamma N}, \\
\tilde{A}_{\Gamma\Gamma} &= A_{\Gamma\Gamma} + \gamma\tilde{H}_{\Gamma\Gamma}, \\
\tilde{B}_{\Gamma\Gamma} &= B_{\Gamma\Gamma} + \gamma\tilde{B}_{\Gamma\Gamma}, \\
\tilde{\mathbf{u}}_\Gamma^0 &= \mathbf{u}_\Gamma^0 + \gamma\mathbf{t}_\Gamma^0,
\end{aligned} \tag{13}$$

and γ is a complex number. If the boundary Γ is a free surface, which corresponds to karstic voids, we have $\mathbf{t}_\Gamma = \mathbf{0}$. Equation (12) reduces to

$$\frac{1}{2}\mathbf{u}_\Gamma = -\tilde{A}_{\Gamma N}\mathbf{u}_N + \tilde{B}_{\Gamma N}\mathbf{t}_N - \tilde{A}_{\Gamma\Gamma}\mathbf{u}_\Gamma + \mathbf{u}_\Gamma^0 \tag{14}$$

from which we can eliminate $\mathbf{u}_\Gamma$ from equation (9) to obtain a matrix relation between boundary values, $\mathbf{u}_N$ and $\mathbf{t}_N$:

$$\mathbf{u}_N = C_{NN}\mathbf{t}_N + \mathbf{b}_N^0 \tag{15}$$

It is proved that if the imaginary part of γ is greater than zero, the relation is unique and stable (e.g., Burton and Miller, 1971b; Colton and Kress, 1983). In the following, we will show that for boundary i, we also have:

$$\mathbf{u}_i = C_{ii}\mathbf{t}_i + \mathbf{b}_i^0 \tag{16}$$

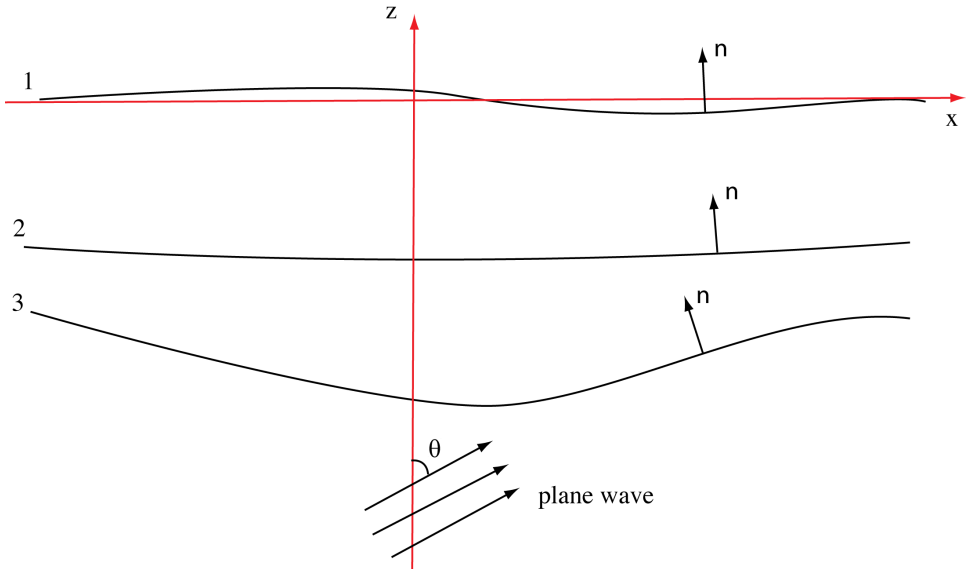

Figure 2. Water layer and definition of surface normal at interface 2.

3.2 Intermediate Layer *m*

The BEM equation for layer m is (we use M to denote m-th interface; and N for the lower (m+1)-th interface)

$$\frac{1}{2}\mathbf{u}_M = -A_{MM}\mathbf{u}_M + B_{MM}\mathbf{t}_M - A_{MN}\mathbf{u}_N + B_{MN}\mathbf{t}_N - A_{M\Gamma}\mathbf{u}_\Gamma + \mathbf{u}_M^0 \qquad (17)$$

$$\frac{1}{2}\mathbf{u}_N = -A_{NM}\mathbf{u}_M + B_{NM}\mathbf{t}_M - A_{NN}\mathbf{u}_N + B_{NN}\mathbf{t}_N - A_{N\Gamma}\mathbf{u}_\Gamma + \mathbf{u}_N^0 \qquad (18)$$

where $\mathbf{u}_M^0$ and $\mathbf{u}_N^0$ are incident field on interfaces M and N, respectively, due to a source in layer m. For the karsts in layer *m*, we have

$$\frac{1}{2}\mathbf{u}_\Gamma = -\tilde{A}_{\Gamma M}\mathbf{u}_M + \tilde{B}_{\Gamma M}\mathbf{t}_M - \tilde{A}_{\Gamma N}\mathbf{u}_N + \tilde{B}_{\Gamma N}\mathbf{t}_N - \tilde{A}_{\Gamma\Gamma}\mathbf{u}_\Gamma + \tilde{\mathbf{u}}_\Gamma^0\,, \qquad (19)$$

from which we can eliminate $\mathbf{u}_\Gamma$ in both equations (17) and (18). Together with the already known relation for interface N:

$$\mathbf{u}_N = C_{NN}\mathbf{t}_N + \mathbf{b}_N^0 \qquad (20)$$

We can get the relation between $\mathbf{u}_M$ and $\mathbf{t}_M$ for the upper interface:

$$\mathbf{u}_M = C_{MM}\mathbf{t}_M + \mathbf{b}_M^0 \qquad (21)$$

We continue the propagator matrix upward to the first layer ($M=1$) where $\mathbf{t}_1 = \mathbf{0}$ for the free surface. From equation (21), we immediately obtain the displacement $\mathbf{u}_1$ on the free surface. If we know $\mathbf{u}_1$ and $\mathbf{t}_1$, we can obtain $\mathbf{u}_2$ and $\mathbf{t}_2$ as well as the displacement $\mathbf{u}_\Gamma$ on karstic surfaces from equations (17) to (20). By induction, displacement and traction on all boundaries can be obtained. One can use these boundary values to compute the wavefield at any point within the model.

4 Validation of the method and examples

To validate our method, we compare it to the analytical solution for a circular inclusion in an otherwise infinite homogenous medium. The *P* and *S* wave speeds are $\alpha = 1.8$ km/s and $\beta = 1.0$ km, respectively, and the density $\rho = 2000$ kg/m^3. The cavity radius is $R = 1.0$ km. The seismic source (explosion) is a line source at $(x_s, z_s) = (0, -1.2)$ km. The linear geophone array is located at depth $z = z_r = 1.2$ km. The source wavelet is a Ricker with a nominal center frequency $f_0 = 1.0$ Hz. We use 400 elements of equal length for the cylindrical cavity boundary. The hypersingular coupling constant γ at frequency f is $\gamma = 1/(2\pi\rho\beta f)$. We compute the multicomponent seismic wavefield using our BEM approach and compare it with the analytical approach described in the Appendix and they produced same results (Figure 3). Since the BEM method is a frequency-domain method, our highest frequency $f_{\max}$ in computation is

$f_{\max} = 3f_0 = 3.0$ Hz. In this example, the irregular frequencies are covered since the maximum $k_\beta R \sim 2\pi f_{\max} R / \beta = 6\pi \gg 1$.

5 Conclusions

In this paper, we present a flexible propagator-matrix scheme to simulate seismic wave propagation in karstic media with many arbitrarily shaped voids. The exact boundary condition along the void boundary is implemented. Numerical instability caused at the fictitious frequencies is removed by using the Miller-Burton formulation. Analytical solution and numerical solution for the cylindrical karst agree with each other.

6 Acknowledgements

We thank Kuwait Foundation for the Advancement of Sciences and Kuwait-MIT Center for Natural Resources and the Environment for support to carry out this research. We also thank Earth Resources lab for facilities support.

References

Benites, R. A., P. M. Roberts, K. Yomogida, and M. Fehler (1997), Scattering of elastic waves in 2-D composite media .1. Theory and test, *Phys. Earth Planet. Inter.*, ***104***(1-3), 161-173.

Bielak, J., R. C. Maccamy, and X. Zeng (1995), Stable Coupling Method for Interface Scattering Problems by Combined Integral Equations and Finite Elements, *Journal of Computational Physics*, ***119***(2), 374-384.

Bouchon, M., and M. Campillo (1989), A boundary integral equation-discrete wavenumber representation method to study wave propagation in multilayered media having irregular interfaces, *Geophysics*, ***54***(9), 1134-1140.

Burton, A. J., and G. F. Miller (1971a), Application of Integral Equation Methods to Numerical Solution of Some Exterior Boundary-Value Problems, *Proceedings of the Royal Society of London Series a-Mathematical and Physical Sciences*, ***323***(1553), 201-&.

Burton, A. J., and G. F. Miller (1971b), The Application of Integral Equation Methods to the Numerical Solution of Some Exterior Boundary-Value Problems, *Proceedings of the Royal Society of London. A. Mathematical and Physical Sciences*, ***323***(1553), 201-210.

Chen, T. R., M. Fehler, X. D. Fang, X. F. Shang, and D. Burns (2012), SH wave scattering from 2-D fractures using boundary element method with linear slip boundary condition, *Geophys. J. Int.*, ***188***(1), 371-380.

Colton, D., and R. Kress (1983), *Integral Equation Methods in Scattering Theory*, 271 pp., John Wiley & Sons, Inc., New York.

Ge, Z. (2010), Simulation of the seismic response of sedimentary basins with constant-gradient velocity along arbitrary direction using boundary element method: SH case, *Earthquake Science*, ***23***(2), 149-155.

Ge, Z., and X. Chen (2007), Wave Propagation in Irregularly Layered Elastic Models: A Boundary Element Approach with a Global Reflection/Transmission Matrix Propagator, *Bull. Seismol. Soc. Am.*, ***97***(3), 1025-1031.

Ge, Z., and X. Chen (2008), An Efficient Approach for Simulating Wave Propagation with the Boundary Element Method in Multilayered Media with Irregular Interfaces, *Bull. Seismol. Soc. Am.*, ***98***(6), 3007-3016.

Ge, Z., L.-Y. Fu, and R.-S. Wu (2005), P-SV wave-field connection technique for regional wave propagation simulation, *Bull. Seismol. Soc. Am.*, ***95***(4), 1375-1386.

Gelis, C., D. Leparoux, J. Virieux, A. Bitri, S. Operto, and G. Grandjean (2005), Numerical modeling of surface waves over shallow cavities, *J Environ Eng Geoph*, ***10***(2), 111-121.

Liu, E., A. Dobson, D. M. Pan, and D. H. Yang (2008), The Matrix Formulation of Boundary Integral Modeling of Elastic Wave Propagation in 2d Multi-Layered Media with Irregular Interfaces, *Journal of Computational Acoustics*, ***16***(3), 381-396.

Liu, E., J. H. Queen, Z. J. Zhang, and D. Chen (2000a), Simulation of multiple scattering of seismic waves by spatially distributed inclusions, *Science in China Series E-Technological Sciences*, ***43***(4), 387-394.

Liu, E. R., and Z. J. Zhang (2000), Elastodynamic bem modelling of multiple scattering of elastic waves by spatial distributions of inclusions, *J Chin Inst Eng*, ***23***(3), 357-368.

Liu, E. R., and Z. J. Zhang (2001), Numerical study of elastic wave scattering by cracks or inclusions using the boundary integral equation method, *Journal of Computational Acoustics*, ***9***(3), 1039-1054.

Liu, Y., R.-S. Wu, and C. F. Ying (2000b), Scattering of elastic waves by an elastic or viscoelastic cylinder, *Geophys. J. Int.*, ***142***(2), 439-460.

Liu, Y. J., and F. J. Rizzo (1993), Hypersingular Boundary Integral-Equations for Radiation and Scattering of Elastic-Waves in 3 Dimensions, *Computer Methods in Applied Mechanics and Engineering*, ***107***(1-2), 131-144.

Martin, P. A. (1990), On the Scattering of Elastic-Waves by an Elastic Inclusion in 2 Dimensions, *Q J Mech Appl Math*, ***43***, 275-291.

Martin, P. A. (2006), *Multiple Scattering: Interaction of Time-Harmonic Waves with N Obstacles*, Cambridge University Press, New York.

Pao, Y. H., and C. C. Mow (1973), *Diffraction of Elastic Waves and Dynamic Stress Concentrations*, 694 pp., Crane Russak, New York.

Pointer, T., E. R. Liu, and J. A. Hudson (1998), Numerical modelling of seismic waves scattered by hydrofractures: application of the indirect boundary element method, *Geophys. J. Int.*, ***135***(1), 289-303.

Rodriguez-Castellanos, A., F. J. Sanchez-Sesma, F. Luzon, and R. Martin (2006), Multiple scattering of elastic waves by subsurface fractures and cavities, *Bull. Seismol. Soc. Am.*, ***96***(4), 1359-1374.

Sanchez-Sesma, F. J., and M. Campillo (1991), Diffraction of P, SV, and Rayleigh waves by topographic features: a boundary integral formulation, *Bull. Seismol. Soc. Am.*, ***81***(6), 2234-2253.

Xia, J., J. Nyquist, Y. Xu, and M. Roth (2006a), Feasibility of Detecting Voids with Rayleigh?Wave Diffraction, in *Symposium on the Application of Geophysics to Engineering and Environmental Problems 2006*, edited, pp. 1168-1180, Society of Exploration Geophysicists.

Xia, J., Y. Xu, R. Miller, and J. Nyquist (2006b), Rayleigh-wave diffractions due to a void in the layered half space, in *SEG Technical Program Expanded Abstracts 2006*, edited, pp. 1406-1410, Society of Exploration Geophysicists.

Yomogida, K., R. Benites, P. M. Roberts, and F. Fehler (1997), Scattering of elastic waves in 2-D composite media II. Waveforms and spectra, *Phys. Earth Planet. Inter.*, ***104***(1-3), 175-192.

Zeng, C., J. Xia, R. Miller, and G. Tsoflias (2012), An improved vacuum formulation for 2D finite-difference modeling of Rayleigh waves including surface topography and internal discontinuities, *Geophysics*, ***77***(1), T1-T9.

Zheng, Y. (2010), Retrieving the exact Green's function by wavefield crosscorrelation, *J. Acoust. Soc. Am.*, ***127***(3), EL93-EL98.

Appendix: Elastic wave scattering by a cylindrical void

For a cylindrical void along the y-direction, embedded in a homogeneous medium, the scattering can be readily computed. Assume the void of radius *R* is centered at $(x,z)=(0,0)$; the point source (line source in 2D) is located at (x_s,z_s) in Cartesian coordinates and in polar coordinates (r_0,ϕ_0). We use α, β and ρ to denote the *P*, *S* wave speeds and density, respectively. We use standard potential method here (e.g., Pao and Mow, 1973; Liu *et al.*, 2000b). Liu *et al.* (2000b) considered plane-wave incidence. Here we give results for the point source excitation. The P-wave potential can be expanded into summation of different angular orders m:

$$\Phi(r,\phi)=\sum_{m=-\infty}^{\infty}\left[\Phi_m^{inc}(r,\phi)+\Phi_m^{scatt}(r,\phi)\right]. \tag{22}$$

Similarly for the S-wave potential we have the following expansion

$$\Psi(r,\phi)=\sum_{m=-\infty}^{\infty}\Psi_m^{scatt}(r,\phi). \tag{23}$$

Since the wavefields for different orders are independent, we consider the case for order m. At order *m*, the incident *P*-wave potential is

$$\Phi_m^{inc}(r,\phi)=\frac{i}{4}J_m(k_\alpha r)H_m(k_\alpha r_0)e^{im(\phi-\phi_0)} \tag{24}$$

and the scattered *P*-wave potential is

$$\Phi_m^{scatt}(r,\phi)=B_m H_m(k_\alpha r)e^{im\phi} \tag{25}$$

and the scattered *SV*-wave potential is

$$\Psi_m^{scatt}(r,\phi)=C_m H_m(k_\beta r)e^{im\phi} \tag{26}$$

where $k_\alpha=\omega/\alpha$ is the *P*-wave background wavenumber, and $k_\beta=\omega/\beta$ the *S*-wave background wavenumber. The displacement field $\mathbf{U}^{(m)}$ can be computed as gradient of the potential fields

$$\mathbf{U}^{(m)}(r,\phi)=\nabla\left(\Phi_m^{inc}+\Phi_m^{scatt}\right)+\nabla\times\left(0,0,\Psi_m^{scatt}\right) \tag{27}$$

in cylindrical coordinates. With this we can compute traction $\mathbf{T}^{(m)}(R,\phi)$ along the karst boundary. The traction should be zero, i.e., $\mathbf{T}^{(m)}(R,\phi)=\mathbf{0}$, in both radial and tangential directions which form two equations from which we can solve for B_m and C_m:

$$\begin{bmatrix} -\left(\rho\omega^2R^2-2\mu m^2\right)-2\mu\chi_m(k_\alpha R) & -2i\mu m\left[1-\chi_m(k_\beta R)\right] \\ -2i\mu m\left[1-\chi_m(k_\alpha R)\right] & \left(\rho\omega^2r^2-2\mu m^2\right)+2\mu\chi_m(k_\beta R)\end{bmatrix}\begin{bmatrix} B_m H_m(k_\alpha R) \\ C_m H_m(k_\beta R)\end{bmatrix} \tag{28}$$

$$=\frac{i}{4}J_m(k_\alpha R)\begin{bmatrix} -\left(\rho\omega^2R^2-2\mu m^2\right)-2\mu\sigma_m(k_\alpha R) \\ -2i\mu m\left[1-\sigma_m(k_\alpha R)\right]\end{bmatrix}$$

where

$$\chi_m(z)=zH_m'(z)/H_m(z) \tag{29}$$

and

$$\sigma_m(z) = zJ_m'(z)/J_m(z) \quad . \tag{30}$$

From equations (28) we can solve for B_m and C_m for order m. The displacement for order m can be then computed using equation (27). The total displacement field $\mathbf{u}$ is the sum of all orders $\mathbf{U}^{(m)}$:

$$\mathbf{u}(r,\phi) = \sum_{m=-\infty}^{\infty} \mathbf{U}^{(m)}(r,\phi) \, . \tag{31}$$

We note that direct computation of (29) and (30) for high-frequency waves at large m may not be numerically stable. However, using basic properties of Bessel (including Hankel) functions, we found the following recursive calculation for $\chi_m(z)$ (also true for $\sigma_m(z)$)

$$\chi_{m+1}(z) = \frac{z^2}{m - \chi_m(z)} - (m+1) \, , \tag{32}$$

whose value at any order *m* can be built from the value $\chi_0(z)$.

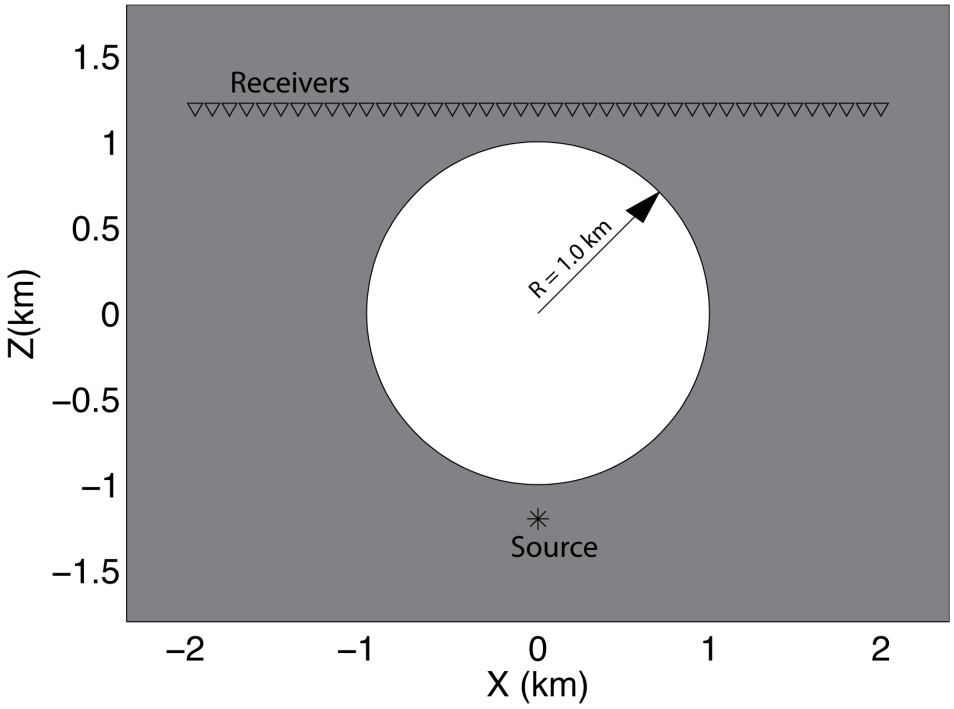

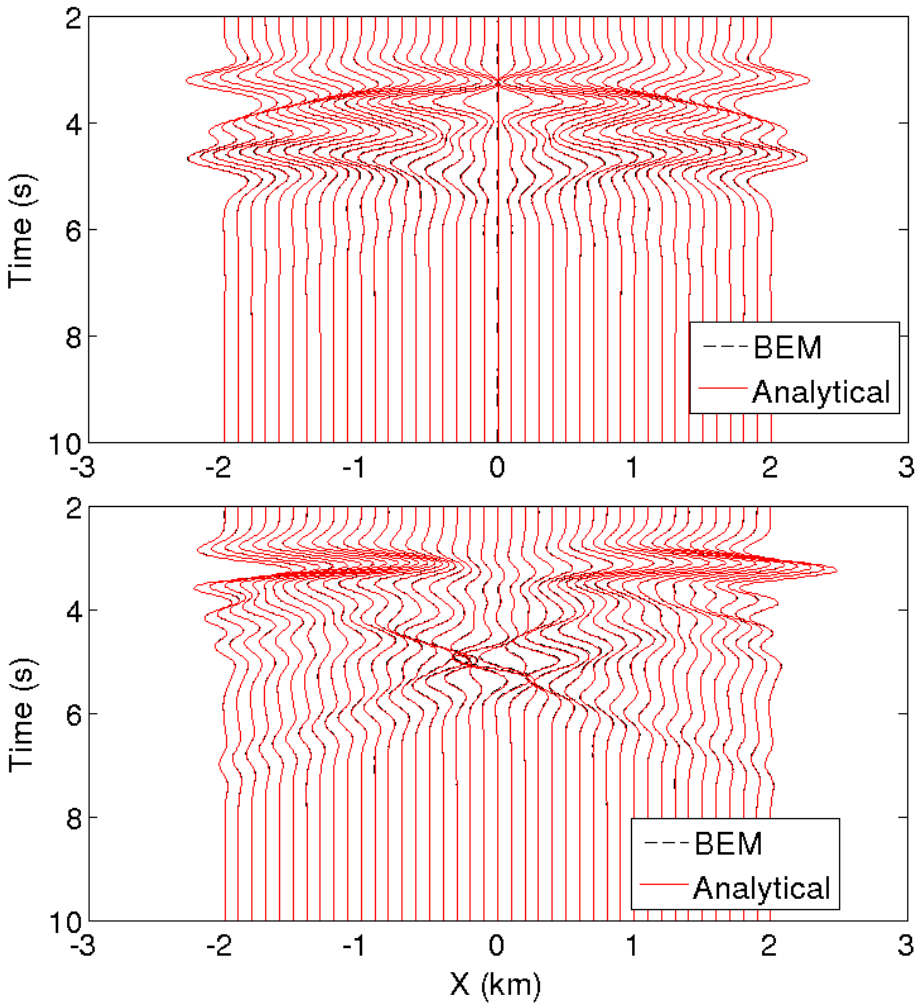

Figure 3. Cavity model (top) with source (star) and receivers (triangles); and waveform comparison between our BEM method and the analytical solution for X- (middle) and Z-component (bottom).